

Anisotropy of the superconducting state properties and phase diagram of MgB₂ by torque magnetometry on single crystals

M. Angst^a, R. Puzniak^b, A. Wisniewski^b, J. Roos^c, H. Keller^c, P. Miranović^d, J. Jun^a, S. M. Kazakov^a, and J. Karpinski^a

^aSolid State Physics Laboratory ETH, 8093-Zürich, Switzerland

^bInstitute of Physics, Polish Academy of Sciences, Aleja Lotnikow 32/46, 02-668 Warsaw, Poland

^cPhysik-Institut, Universität Zürich, 8057 Zürich, Switzerland

^dDepartment of Physics, Okayama University, 700-8530 Okayama, Japan

The angular and temperature dependence of the upper critical field H_{c2} in MgB₂ was determined from torque magnetometry measurements on single crystals. The H_{c2} anisotropy γ_H was found to decrease with increasing temperature, in disagreement with the anisotropic Ginzburg-Landau theory, which predicts that the γ_H is temperature independent. This behaviour can be explained by the two band nature of superconductivity in MgB₂. An analysis of measurements of the reversible torque in the mixed state yields a field dependent effective anisotropy γ_{eff} , which can be at least partially explained by different anisotropies of the penetration depth and the upper critical field. It is shown that a peak effect in fields of about $0.85 H_{c2}$ is a manifestation of an *order-disorder* phase transition of vortex matter. The H - T phase diagram of MgB₂ for $H\parallel c$ correlates with the intermediate strength of thermal fluctuations in MgB₂, as compared to those in high and low T_c superconductors.

1. Introduction

Superconducting MgB₂ exhibits a number of rather peculiar properties, originating from the involvement of two sets of bands of different anisotropy and different coupling to the most relevant phonon mode [1,2]. Among them are pronounced deviations of the upper critical field, H_{c2} , from predictions of the widely used anisotropic Ginzburg-Landau theory (AGLT).

Apart from two-band superconductivity, MgB₂ provides a link between low and high T_c superconductors on a phenomenological level, particularly concerning vortex physics. In both high and low T_c superconductors, for example, a phase transition of vortex matter out of a quasi-ordered “Bragg glass” have been identified, with rather different positions in the H - T plane. Studying the intermediate MgB₂ may help establishing a “universal vortex matter phase diagram”.

Here, we present a torque magnetometry study of the anisotropic upper critical field, equilibrium magnetization, and the vortex matter phase dia-

gram of single crystalline MgB₂ [3]. We will show direct evidence of a temperature dependence of the H_{c2} anisotropy, discuss strong indications of a difference between the anisotropies of the penetration depth and H_{c2} , and present the H - T phase diagram for $H\parallel c$.

Single crystals were grown with a cubic anvil high pressure technique, described in this issue [4]. Three crystals were used in this study, labeled A, B, and C. Sharp transitions to the superconducting state indicate a high quality of the crystals. An $M(T)$ curve of crystal B with $T_c = 38.2$ K can be found in Ref. [5].

The torque $\vec{\tau} = \vec{m} \times \vec{B} \simeq \vec{m} \times \vec{H}$, where \vec{m} is the magnetic moment of the sample, was recorded as a function of the angle θ between the applied field \vec{H} and the c -axis of the crystal in various fixed fields [6]. For measurements close to T_c , in fields up to 14 kOe, a non-commercial magnetometer with very high sensitivity was used [7]. For part of these measurements, a vortex-shaking process was employed to speed up the relaxation of the vortex lattice [8]. Crystal A was measured in this

system. Crystals B and C were measured in a wider range of temperatures down to 14 K, in a Quantum Design PPMS with torque option and a maximum field of 90 kOe. For crystals B and C, $\tau(H)$ measurements at fixed angles were performed in addition to $\tau(\theta)$ measurements in fixed H .

2. Upper critical field and it's anisotropy

Early measurements on polycrystalline or thin film MgB₂ samples with various methods and single crystals by electrical transport yielded values of the anisotropy parameter of the upper critical field $\gamma_H = H_{c2}^{\parallel ab}/H_{c2}^{\parallel c}$ in a wide range of values of $1.1 \leq \gamma_H \leq 9$ [9]. More recently, several papers reported a temperature dependence of the H_{c2} anisotropy, ranging between about 5–8 at 0 K and 2–3 close to T_c [10,11,12,13,14,15,16,17,18]. In this section, we present direct evidence of a temperature dependence of the H_{c2} anisotropy γ_H and discuss details of it's behaviour, comparing the torque data with numerical calculations [19].

Four angular torque dependences are shown in Fig. 1. Panels a) and b) correspond to measurements at 22 K. For fields nearly parallel to the c -axis, both curves are flat, apart from a small background visible in panel b). Only when H is nearly parallel to the ab -plane there is an appreciable torque signal. The curve can be interpreted in a straight-forward way: for H parallel to the c -axis the sample is in the normal state, while for H parallel to the ab -plane it is in the superconducting state. The crossover angle θ_{c2} between the normal and the superconducting state is the angle for which the fixed applied field is the upper critical field. From the existence of both superconducting and normal angular regions follows immediately that $H_{c2}^{\parallel c}(22 \text{ K}) < 19 \text{ kOe}$ and $85 \text{ kOe} < H_{c2}^{\parallel ab}(22 \text{ K})$. In panel c), on the other hand, the crystal is seen to be in the superconducting state for all values of the angle θ , and therefore $4 \text{ kOe} < H_{c2}^{\parallel c}(34 \text{ K})$. Finally, the data in panel d) show only a small background contribution – form and angular regime of the deviation from a straight line are incompatible with a superconducting signal. Therefore, the crystal is

here in the normal state for any θ , and we have $H_{c2}^{\parallel ab}(34 \text{ K}) < 14 \text{ kOe}$.

From figure 1 we therefore have two limitations for the upper critical field anisotropy, hereafter called γ_H , without any detailed H_{c2} criterion, and without any model fits :

$$\gamma_H(22 \text{ K}) > \frac{85}{19} \simeq 4.47; \quad \gamma_H(34 \text{ K}) < \frac{14}{4} = 3.5. \quad (1)$$

These relations show that *the upper critical field anisotropy γ_H of MgB₂ cannot be temperature independent*. As an immediate implication, the *anisotropic Ginzburg-Landau theory* (AGLT) in it's standard form *does not hold for MgB₂*. The deviation is strong, within a change of temperature of about $0.3 T_c$, γ_H changes, *at least*, by a fifth of it's value.

Although it is clear that AGLT with it's effective mass anisotropy model cannot describe the data measured at *different* temperatures consistently, the detail analysis of the θ dependence of H_{c2} we used is based on AGLT. We will show that as long as we stay at a *fixed* temperature, AGLT is able to describe $H_{c2}(\theta)$ remarkably well [20]. Although the location of θ_{c2} , for example in Fig. 1a), seems clear at first sight, this clarity disappears, when examining the transition region in a scale necessary for the precise determination of θ_{c2} (see Fig. 1 in Ref. [10]). For an strict analysis, it is necessary to take into account that the transtion at H_{c2} is rounded off by fluctuations.

In sufficiently high fields, $H > H_{LLL}$, the so-called “lowest Landau level” (LLL) approximation was used successfully to describe the effects of fluctuations around H_{c2} [21,22]. In the case of the cuprates, the value of H_{LLL} , and thus of the regime of applicability of the LLL approximation, is a controversial issue (see, e.g., Ref. [23] for a theoretical discussion of the limits of the LLL approximation). However, in the case of MgB₂, even using the theoretical criterion of Ref. [23], which led to the high estimation $H_{LLL} \approx 200 \text{ kOe}$ in the case of YBa₂Cu₃O_{7- δ} , we obtain an upper limit of $H_{LLL} \approx 5 \text{ kOe}$. We therefore used a LLL scaling analysis for the determination of $\theta_{c2}(H)$ or $H_{c2}(\theta)$ [10].

From the resulting $H_{c2}(\theta)$ curve, the anisotropy parameter γ_H is then extracted by an analysis

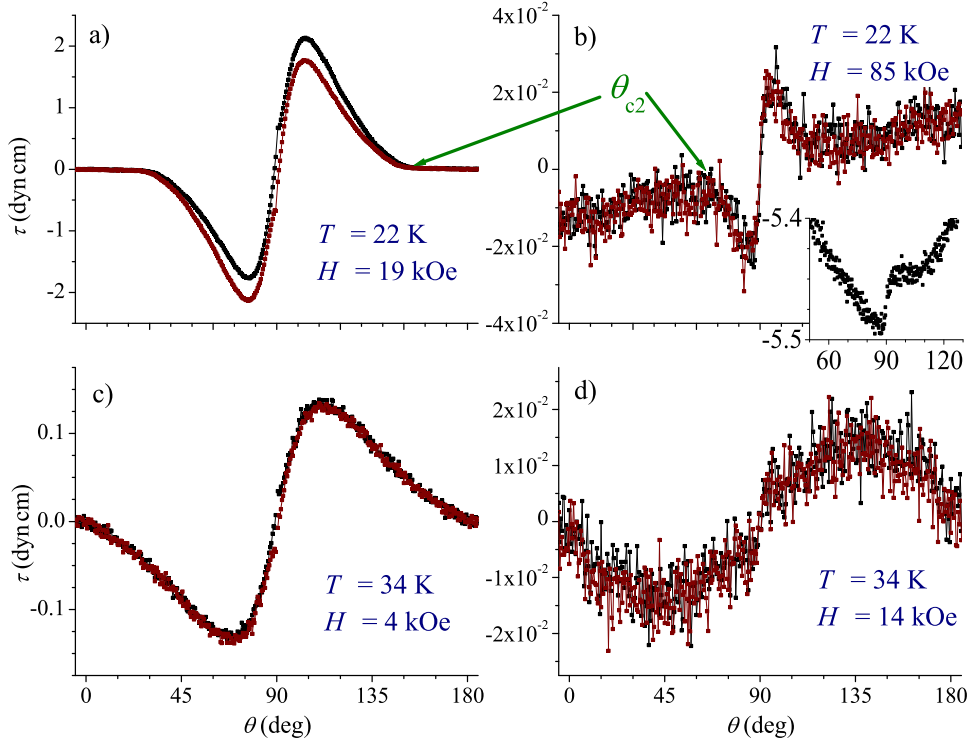


Figure 1. Torque τ vs. angle θ of MgB₂ single crystal B. The raw data have been antisymmetrized around 90 deg in order to subtract a symmetric background (which was of the order of 0.05–0.2 dyn cm, depending on H and T). θ_{c2} indicates the angle for which the applied field is the upper critical field. The schematic drawing in a) shows the definition of the angle θ . The inset in b) shows the data before antisymmetrizing.

with AGLT, which predicts the angular dependence of the upper critical field to be [24]

$$H_{c2}(\theta) = H_{c2}^{\parallel c} (\cos^2 \theta + \sin^2 \theta / \gamma_H^2)^{-1/2}. \quad (2)$$

We note that in the rescaling of the torque according to the LLL fluctuations theory, the target parameter γ_H is used, which is obtained only later with Eq. (2). Therefore, scaling analysis and determination of γ_H with Eq. (2) had to be performed iteratively in order to self consistently find γ_H . However, the $\theta_{c2}(H)$ and $H_{c2}(\theta)$ points obtained with the scaling analysis depend not very strongly on the value of γ_H used in the scaling and the procedure converges rather fast.

Figure 2 shows the angular dependence of H_{c2}

of crystal B and C. The curves shown in the figure are fits of Eq. (2) to the data, showing that the angular dependence of H_{c2} is well described by AGLT at both temperatures. On the other hand, the anisotropy parameter γ_H needed to describe the data with Eq. (2) is temperature dependent, as is best seen in the inset.

The irreversible properties of the two crystals (B and C) are different in a pronounced way (see Secs. 3 and 4), showing that they have a rather different defect structure. The good agreement both in value and angular dependence of H_{c2} of crystals B and C that is observable in Fig. 2 indicates that such differences in the defect structure do not influence the upper critical field much,

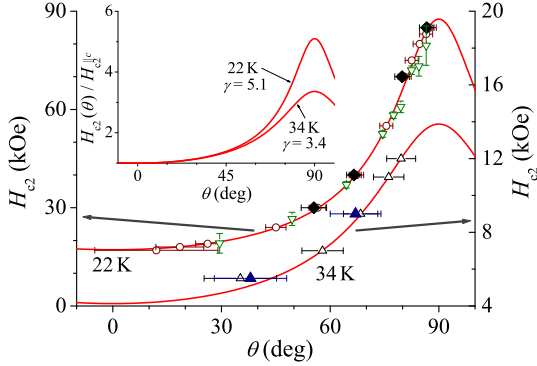


Figure 2. Comparison of $H_{c2}(\theta)$ dependence of crystals B and C, at 22 and 34 K. Shown are results obtained both from $\tau(\theta)$ measurements in fixed H [B at 22 K (\circ) and at 34 K (\triangle), C at 22 K (\blacklozenge) and at 34 K (\blacktriangle)] and from $\tau(H)$ measurements at fixed θ [B at 22 K (∇)]. Inset: calculated curves from the main panel, scaled to the fitted value of $H_{c2}^{\parallel c}$.

at least in the region between 22 and 34 K, and therefore cannot influence our conclusion of a T dependent H_{c2} anisotropy.

Small, but systematic, deviations from the angular dependence of H_{c2} according to Eq. (2) were observed only at temperatures close to T_c . It may indicate that we are approaching H_{LLL} in this region and the values of $\theta_{c2}(H)$ and $H_{c2}(\theta)$ obtained from the LLL scaling analysis (see above) start to deviate from the mean field values. The good general approximation of $H_{c2}(\theta)$ by Eq. (2) is in agreement with recent calculations [19]. However, the calculations predict small deviations at low temperatures [25], rather than close to T_c . Our experimental limitation of fields up to 90 kOe may prevent the observation of deviations from Eq. (2) at low temperatures.

The upper critical fields parallel and perpendicular to the layers obtained with the scaling analysis and Eq. (2) are shown in Fig. 3a). Results obtained for two crystals measured in two magnetometers are depicted as different symbols. The T -dependence of $H_{c2}^{\parallel c}$ is in agree-

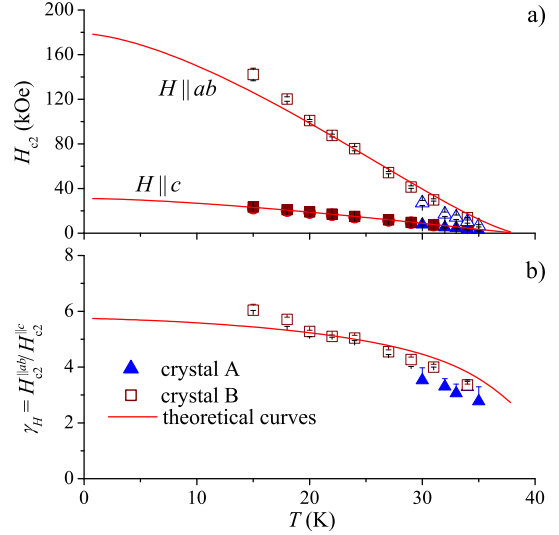


Figure 3. a) Upper critical field H_{c2} vs. temperature T . Open symbols correspond to $H \parallel ab$, full symbols to $H \parallel c$, from fits of Eq. (2) to the $H_{c2}(\theta)$ data. Up triangles are from measurements on sample A (with θ_{c2} determined with a simple “straight line crossing” criterion) and squares are from measurements on sample B, using a fluctuation analysis (see text). Full lines are theoretical calculated curves [19]. b) Temperature dependence of the upper critical field anisotropy $\gamma_H = H_{c2}^{\parallel ab}/H_{c2}^{\parallel c}$, determined from fits of Eq. (2) to $H_{c2}(\theta)$. The full line is again from the theoretical calculation of Ref. [19].

ment with (isotropic) calculations by Helfand *et al.* [26], with $H_{c2}^{\parallel c}(0) \simeq 31$ kOe. On the other hand, $H_{c2}^{\parallel ab}(T)$ exhibits a slight positive curvature near T_c . These features are common to highly anisotropic (layered) superconductors. Although MgB_2 as a whole is rather isotropic, superconductivity is dominant on the quasi-2D bands, which may well account for the different T dependence of $H_{c2}^{\parallel c}$ and $H_{c2}^{\parallel ab}$. This may also be the origin of the positive curvature of H_{c2} observed in other measurements of bulk, thin film and single crystal MgB_2 [9]. Due to the lack of low T data

and the $\gamma_H(T)$ dependence, only an estimation $180 \text{ kOe} \lesssim H_{c2}^{\parallel ab}(0) \lesssim 230 \text{ kOe}$ can be given.

The anisotropy data [Fig. 3b)] show that γ_H *systematically decreases* with increasing temperature, from $\gamma_H \simeq 6$ at 15 K to 2.8 at 35 K. From the experimental data shown in Fig. 3 we estimate $\gamma_H(T_c) = 2.3 - 2.7$, while at zero temperature, γ_H may become as large as 8.

Comparing our data with the data reported by other authors [11,12,13,14,15,16,17,18], we note that electrical transport measurements [14,15] yield too high values of $H_{c2}^{\parallel c}$ [11,13]. All bulk measurements (torque [10], magnetization [12,13,16,18], thermal conductivity [11], and specific heat [13,17]) agree well on the $H_{c2}^{\parallel c}(T)$ dependence and value. Concerning $H_{c2}^{\parallel ab}(T)$, and consequently $\gamma_H(T)$, however, reported values differ from each other. Exchanging the samples between different groups could help clarifying, whether the discrepancies of $H_{c2}^{\parallel ab}(T)$ values are mainly due to sample differences or due to differences in the experimental methods employed.

Very recently, $H_{c2}^{\parallel ab}(T)$, $H_{c2}^{\parallel c}(T)$, and $\gamma_H(T)$, have been calculated for MgB_2 [19]. The Fermi surface was modeled as consisting of two separate sheets, approximated as simple spheroids, but with average characteristics taken from first principles calculations. The result of these calculations are compared with our experimental data in Fig. 3. Very good agreement is seen for the upper critical field perpendicular to the layers ($\parallel c$). Qualitatively, calculations and experiment also agree well for the upper critical field parallel to the layers ($\parallel ab$). This shows that the essential source of the deviations of the upper critical field from AGLT predictions is captured with a simple effective two band model, while further details of the Fermi surface and superconducting gap are negligible. In Fig. 3, we see good quantitative agreement between experimental data and the theoretical curve between 20 and 25 K.

The deviations at lower T may, on the one hand, be due to a decreased the accuracy of our analysis because the field limitation of 90 kOe restricts the angular range where H_{c2} data could be obtained. This can lead to deviations larger than the estimated error bars, especially since the

theoretical calculations indicate deviations of the $H_{c2}(\theta)$ dependence from the prediction of Eq. (2) at low T [25]. On the other hand, H_{c2} at low temperatures depends on the shape of the Fermi surface in rather subtle manner, and the model Fermi surface used for the calculations [19] may be too simple for a quantitatively correct description at low T . The deviations at higher T may be due to the limitations of the LLL scaling approach in low fields, and or due to the influence of disorder, which is not accounted for in the calculations.

Close to T_c , non-locality is not important, and consequently, AGLT is expected to hold even if this is not the case at lower T . Despite of this, Fig. 3 clearly indicates that the variation of γ_H with temperature is the strongest close to T_c . Therefore, in MgB_2 , AGLT seems to have a very limited range of applicability indeed.

3. Reversible and irreversible torque below H_{c2}

An alternative method to obtain the anisotropy parameter γ of a superconductor, used often and with success in the case of cuprates [8,27,28], consists of measuring the torque, as a function of angle, well below H_{c2} , and analyzing the data with a formula developed by Kogan [29]:

$$\tau = -\frac{\Phi_0 H V}{64\pi^2 \lambda_{ab}^2} \left(1 - \frac{1}{\gamma_{\text{eff}}^2}\right) \frac{\sin 2\theta}{\epsilon(\theta)} \ln \left(\frac{\eta H_{c2}^{\parallel c}}{\epsilon(\theta) H}\right), \quad (3)$$

where $\epsilon(\theta) = (\cos^2 \theta + \sin^2 \theta / \gamma_{\text{eff}}^2)^{1/2}$, $\gamma_{\text{eff}} = (m_c^*/m_{ab}^*)^{1/2}$ is the effective mass anisotropy, λ_{ab} is the in-plane penetration depth, V is the volume of the crystal, Φ_0 is the flux quantum, and η is a constant of the order of unity depending on the vortex lattice structure. Equation (3) is valid in the limits of fields $H_{c1} \ll H \ll H_{c2}$ and not too close to T_c . A further restriction is that Eq. (3) describes the reversible torque only. To obtain the true reversible torque, we employed a vortex-shaking process [8]. In the investigated field and temperature region, the shaken torque was found to be well reversible.

In Fig. 4, normalized torque τ/τ_{max} vs angle θ curves, measured in different fields at 34 K, are compared. Increasing H from 2 [panel a)] to

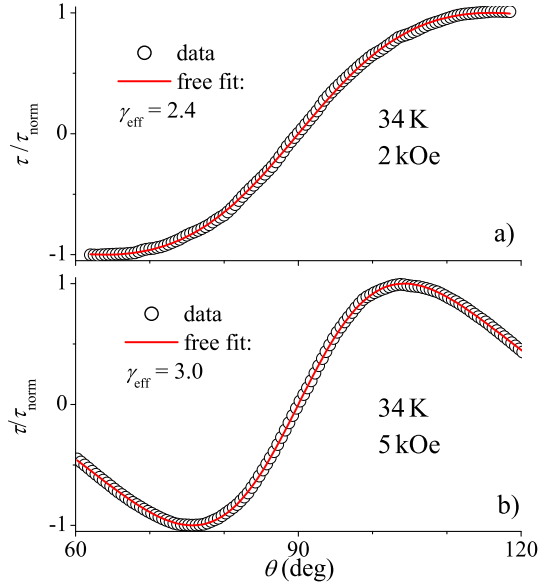


Figure 4. Normalized reversible torque vs angle at 34 K in 2 kOe [a] and 5 kOe [b]. Shown together with the measured values (open circles) are best fits of Eq. (3) (full curves).

5 kOe [panel b]) leads to an unexpectedly large shift of the maximum torque towards 90 deg, which may indicate an increase of the anisotropy γ_{eff} with increasing H . This is confirmed by the analysis of the data with Eq. (3). The best agreements of the equation with the data are obtained for $\gamma_{\text{eff}} = 2.4$ in 2 kOe and $\gamma_{\text{eff}} = 3.0$ in 5 kOe (full curves in Fig. 4). Although descriptions with $\gamma_{\text{eff}} = 3.0$ in 2 kOe or $\gamma_{\text{eff}} = 2.4$ in 5 kOe are also possible without obvious discrepancies to the data, the corresponding qualities of the fit as expressed by the parameter χ^2 are worse by more than an order of magnitude in both cases.

From the analysis of reversible torque data for crystal A measured in the range of fields and temperatures from 1 to 10 kOe and from 27 to 36 K [10], a few points are worth to be emphasized: 1.) γ_{eff} is field dependent, increasing nearly linearly from 2 in zero field to 3.7 in 10 kOe. 2.) No clear T dependence is visible between 27 and

36 K. 3.) The effective anisotropy γ_{eff} , as obtained from the analysis with Eq. (3) is different from the H_{c2} anisotropy γ_H .

Especially concerning point 3.), it is important to recognize that, also theoretically, the anisotropy γ_{eff} is not necessarily the same as the H_{c2} anisotropy γ_H . When AGLT is not applicable, the anisotropies of the penetration depth, γ_λ , and of the upper critical field, γ_H , differ in general. Calculations of γ_λ of MgB₂ [30,31] indeed found values much lower than the upper critical field anisotropy values. There is also experimental support for a low γ_λ [32].

In Eq. (3), γ_{eff} appears twice, and in a first approximation [33], the appearance outside of the logarithm can be thought of as due to the λ anisotropy, while the appearance in the logarithm is linked to the H_{c2} anisotropy. A corresponding calculation with different (fixed) γ_λ and γ_H yields [34] a field dependent (common) effective anisotropy γ_{eff} similar to the experimental observations.

Field dependent point-contact spectroscopy [35] and specific heat [36] measurements indicate that the small gap disappears in fields of the order of 4–5 kOe, i.e., superconductivity in the (3D) π Fermi sheets is rapidly suppressed by even low fields, whereas it persists in the (2D) σ sheets up to much higher fields. This should result in an increase of the effective (bulk) anisotropy with increasing H . Further studies are needed for a complete understanding of the detailed interplay of the effects described above.

In the “unshaked” torque data of crystals A and B, a pronounced peak in the irreversible torque for field alignments close to $H\|ab$, was observed (see, e.g., upper inset of Fig. 5 of Ref. [10]). It is tempting to ascribe this feature, also observed by other authors [37], to “intrinsic pinning”, in analogy to observations on strongly anisotropic cuprate superconductors. However, the observation of such “intrinsic pinning” in MgB₂ is rather counter-intuitive, since the “intrinsic pinning” is mostly determined by the ratio of the c -axis coherence length to the separation of the superconducting layers, which is much larger in MgB₂ than in the case of cuprates in the region where “intrinsic pinning” is commonly observed

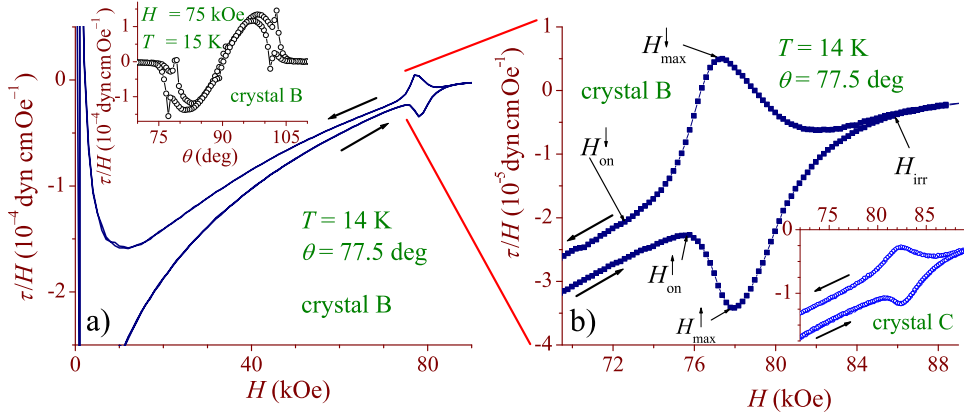


Figure 5. Torque τ/H vs field H at 14 K and 77.5 deg. a) Full curve for crystal B. The direction of the field change is indicated by arrows. Inset: τ/H vs angle θ in 75 kOe at 15 K (crystal B) b) magnification of the peak effect region of crystal B. The irreversibility field H_{irr} and the onset and maximum fields H_{on} and H_{max} of the PE for the H increasing (\uparrow) and decreasing (\downarrow) branch are marked. Inset: Curve obtained under the same external conditions for crystal C.

by torque magnetometry (see, e.g., [28]). The apparent paradox is resolved by further measurements: torque measurements on crystal C with the same conditions show no sign of “intrinsic” pinning for $H \parallel ab$ [38,34], indicating the *extrinsic* origin of the feature. The most likely cause of the peak in the irreversible torque for $H \parallel ab$ is a small amount of stacking faults. It may indicate the presence of some stacking faults in crystals A and B, while they would seem to be absent in crystal C [39].

4. Peak effect and vortex matter phase diagram

In low T_c superconductors, such as NbSe $_2$, the order-disorder transition is signified experimentally by a peak effect (PE) in the critical current density [40]. We observed such a PE by torque measurements on MgB $_2$ single crystals B and C, both in $\tau(\theta)$ and $\tau(H)$ measurements, as can be seen in Fig. 5. In Sec. 3, we have noticed that crystals B and C behave quite differently for $H \parallel ab$, which may be due to the presence of a small number of stacking faults in the former one. The presence of the PE in two crystals with such

pronounced differences strongly indicates that the PE, or rather it’s underlying mechanism, is an intrinsic feature of MgB $_2$. A study with a “minor hysteresis loop” technique on crystal B [5] revealed a history dependent critical current density in the PE region, compatible with and expected for the behaviour at the order-disorder transition.

Figure 6 shows the irreversible part $\Delta\tau(H) = \tau(H^{\downarrow}) - \tau(H^{\uparrow})$ of the torque, scaled by $H \sin 2\theta$, vs field, at 18 K for various angles. The scaling was chosen to minimize the angle and field dependence intrinsic to the torque. Since the peak is not visible at all temperatures and angles as well as in Fig. 5, onsets and maxima were determined from irreversible torque curves as those shown in Fig. 6. H_{on} was defined as the field, where the irreversible torque starts to deviate from a straight line behaviour, as indicated in the figure for the curve measured at 71.5 deg. H_{on} , defined in this way, is close to $H_{\text{on}}^{\downarrow}$ as indicated in Fig. 5b). However, we note that with the determination of onsets and maxima from the irreversible torque, the fine details of the differences in the field increasing and decreasing branch of the hysteresis loops

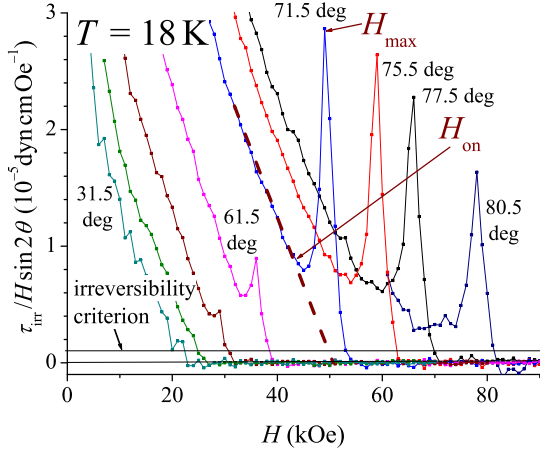


Figure 6. Variation of the irreversible torque, scaled by $H \sin 2\theta$, vs field, at 18 K. Shown are representative curves, measured at angles (from left to right) $\theta = 31.5, 41.5, 51.5, 61.5, 71.5, 75.5, 77.5$, and 80.5 deg. Horizontal lines indicate zero and the criterion of 10^{-6} dyn cm Oe $^{-1}$ chosen for the determination of the irreversibility line. For the curve measured at 71.5 deg, peak maximum and onset are indicated (see text).

are lost.

It can be seen in Fig. 6 that the height of the peaks varies in a pronounced way with the angle θ . One possible explanation for this behaviour is an interaction of the peak effect with stacking faults [39]. Although the presence and the location of the peak effect are not affected by stacking faults, the extent of hysteresis may be. The difference of how pronounced the peaks of crystals B and C are [see Fig. 5b)] supports such a scenario. The location in higher fields of the peak effect in crystal C indicates that there is less point-like disorder present in this crystal than in crystal B. However, the smaller ratio $\tau_{\text{irr}}(H_{\text{max}})/\tau_{\text{irr}}(H_{\text{on}})$ in crystal C, compared to crystal B, is difficult to explain with only one sort of disorder. Individual strong pinning, e.g., by sparse stacking faults, should be much more efficient in the disordered phase than in the Bragg glass with it's

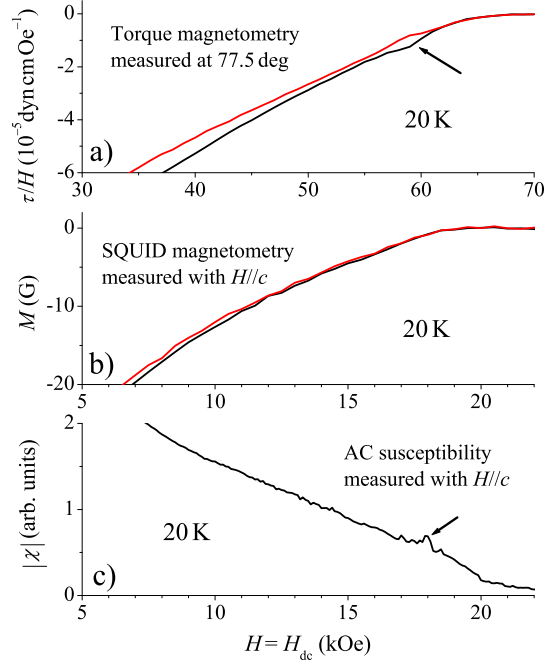


Figure 7. Comparison of different measurement techniques in the peak effect region, at 20 K. a) Torque τ/H vs H , measured at an angle of 77.5 deg between the c -axis of the sample and the applied field. Due to the anisotropy, the location in fields of the PE is much higher than for $H||c$, but the angular scaling is straight forward [5]. b) Magnetization M vs H , for $H||c$, determined by SQUID magnetometry. c) Absolute magnetic susceptibility $|\chi|$ vs $H \equiv H_{\text{dc}}$, measured with an ac amplitude $H_{\text{ac}} = 10$ Oe and a frequency of 10 kHz. The PE visible in panels a) and c) is indicated by arrows.

nearly perfect ordered lattice [41]. If the peak height observed in crystal B is affected by stacking faults, a more pronounced PE close to $H||ab$ is natural, since the pinning efficiency of stacking faults, similar to twin boundary pinning, is strongly direction-dependent [42].

On the other hand, the peak height can be influenced by the natural angle dependence of the torque, despite the scaling made. This is because

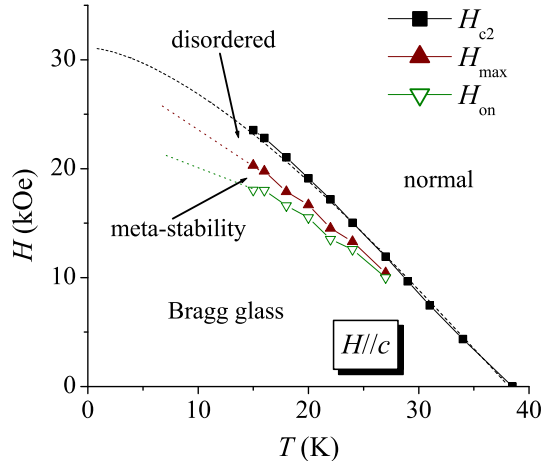


Figure 8. Vortex matter phase diagram of MgB_2 (crystal B) for $H\parallel c$. Data points shown are from the projection of the torque vs field data presented in Ref. [5] and the projection of additional $\tau(\theta)$ measurements in fixed H . The dashed line is a calculation [19] of the H_{c2} dependence (cf. Fig. 3), the dotted lines are guides for the eye. The different phases of vortex matter are labeled (see text).

the $\sin 2\theta$ is only an approximation, which is not appropriate for all angles θ , in a superconductor with pronounced anisotropy (see also Ref. [5]).

The angular dependence of the *onsets and maxima* of the PE tracks the one of H_{c2} , i.e., it follows Eq. (2) [5]. This indicates that the PE (or rather its underlying mechanism) is a feature for all directions of the applied field, and not just of the angular region where it is readily discernible. To directly check the situation for $H\parallel c$ and $H\parallel ab$, where torque measurements are not possible, SQUID and ac susceptibility [43,44] measurements were performed.

In Fig. 7, we compare measurement curves obtained on crystal B at 20 K, using different experimental techniques. Torque measurements performed at an angle of 77.5 deg show [Fig. 7a)] a clearly discernible PE located in a field of about 60 kOe. Scaled with Eq. (2) to $H\parallel c$, this corre-

sponds to 15 to 20 kOe. As can be seen in Fig. 7b), there is no sign of a PE observable in SQUID data in this field region. Generally, no sign of a peak effect was observed by SQUID magnetometry at any temperature, for both field directions. This is likely due to insufficient sensitivity of the SQUID. In ac susceptibility data [Fig. 7c)], on the other hand, a PE *is* visible for $H\parallel c$ in the appropriate field region. A report of the ac susceptibility results will be published elsewhere [44]. A PE in MgB_2 was also reported recently by other authors, in the case of $H\parallel c$ from transport data [13,17] and ac susceptibility with a local Hall probe [17,45], in the case of $H\parallel ab$ from transport data [17].

The phase diagram for $H\parallel c$ obtained from torque magnetometry, based on both $\tau(\theta)$ and $\tau(H)$ measurements and the angular scaling of Eq. (2) is presented in Fig. 8. The magnitude of the peaks is reduced quickly by increasing the temperature, and above 27 K, the PE is no longer discernible in the torque data. This is due to the decreased sensitivity of the torque magnetometer in lower fields and due to thermal smearing of the effective pinning potential. In a recent report of low frequency ac susceptibility measurements [45], the peak effect was observed for $H\parallel c$ at temperatures up to about 25 K, and interpreted in terms of the order-disorder transition as well. In Ref. [45], the transformation of the PE into a “step-like” ac susceptibility is reported for the temperature interval between 25 and 27.5 K, and interpreted as a signature of thermal melting. In our case, no step-like feature in the reversible torque was observed in the continuation of the PE. It should be emphasized, that thermal melting so far below H_{c2} would be at odds [5] with theoretical expectations [46].

The equilibrium order-disorder transition, which corresponds to H_{max} [5], is located in fields of about $0.85 H_{c2}$ in crystal B and in about $0.9 H_{c2}$ in crystal C. The peak effect observed in other crystals by transport was reported to be located even closer to H_{c2} [13,17]. These differences are natural for a disorder-induced phase transition in crystals with varying degrees of disorder. Form and location of the PE observed in MgB_2 resembles results obtained on NbSe_2 single crys-

tals with varying degrees of disorder [40], but are rather different from the order-disorder transition in cuprate superconductors [47].

5. Conclusions

In summary, studying the anisotropic superconducting state properties of MgB_2 revealed a strong temperature dependence of the upper critical field anisotropy γ_H , and indicated a difference of the anisotropies of the penetration depth and the upper critical field. These findings, which imply a breakdown of the standard form of the widely used anisotropic Ginzburg-Landau theory in MgB_2 , can be explained by superconductivity in this compound involving two band systems of different dimensionality, in accordance with microscopic studies.

A pronounced peak effect in the magnetic hysteresis is a signature of an “order-disorder” transition of vortex matter, similar to transitions in both high T_c cuprate and low T_c superconductors. Despite the intermediate importance of thermal fluctuations in MgB_2 , the phase diagram resembles quite closely the one of the low T_c superconductor NbSe_2 . On the other hand, chances of a proper identification of mainly thermally induced melting at higher temperatures are better in MgB_2 , due to the increased thermal fluctuations.

Acknowledgements

We thank V. G. Kogan and B. Batlogg for enlightening and stimulating discussions. This work was supported by the Swiss National Science Foundation, by the European Community (contract ICA1-CT-2000-70018), by the Polish State Committee for Scientific Research (5 P03B 12421), and by the Swiss federal office BBW (02.0362).

REFERENCES

1. A. Y. Liu, I. I. Mazin, and J. Kortus, *Phys. Rev. Lett.* **87**, 087005 (2001).
2. H. J. Choi, D. Roundy, H. Sun, M. L. Cohen, and S. G. Louie, *Nature* **418**, 758 (2002).
3. An extended discussion of the results presented here can be found in M. Angst, PhD thesis, submitted to ETH Zürich.
4. J. Karpinski, S. M. Kazakov, J. Jun, M. Angst, R. Puzniak, A. Wisniewski, and P. Bordet, this issue.
5. M. Angst, R. Puzniak, A. Wisniewski, J. Jun, S. M. Kazakov, and J. Karpinski, *cond-mat/0205293*.
6. Note that there are two torque conventions used in the literature, leading to opposite signs of the torque shown, but to the same physical consequences. The convention used here (and in Refs. [5,8,10,28,34,38]) is that the diamagnetism is expressed by a negative value of the magnetic moment. The other convention, used in Refs. [7,27,33,37], is that the diamagnetism is expressed solely by the direction of the (positive) magnetic moment vector.
7. M. Willemin, C. Rossel, J. Brugger, M. H. Despont, H. Rothuizen, P. Vettiger, J. Hofer, and H. Keller, *J. Appl. Phys.* **83**, 1163 (1998).
8. M. Willemin, C. Rossel, J. Hofer, H. Keller, A. Erb, and E. Walker, *Phys. Rev. B* **58**, R5940 (1998).
9. C. Buzea and T. Yamashita, *Supercond. Sci. Technol.* **14**, R115 (2001).
10. M. Angst, R. Puzniak, A. Wisniewski, J. Jun, S. M. Kazakov, J. Karpinski, J. Roos, and H. Keller, *Phys. Rev. Lett.* **88**, 167004 (2002).
11. A. V. Sologubenko, J. Jun, S. M. Kazakov, J. Karpinski, and H. R. Ott, *Phys. Rev. B* **65**, 180505(R) (2002).
12. S. L. Bud’ko and P. C. Canfield, *Phys. Rev. B* **65**, 212501 (2002).
13. U. Welp, G. Karapetrov, W. K. Kwok, G. W. Crabtree, C. Marcenat, L. Paulius, T. Klein, J. Marcus, K. H. P. Kim, C. U. Jung, H.-S. Lee, B. Kang, and S.-I. Lee, *cond-mat/0203337*.
14. Y. Eltsev, S. Lee, K. Nakao, N. Chikumoto, S. Tajima, N. Koshizuka, and M. Murakami, *Phys. Rev. B* **65**, 140501(R) (2002).
15. C. Ferdeghini, V. Braccini, M. R. Cimberle, D. Marre, P. Manfrinetti, V. Ferrando, M. Putti, and A. Palenzona, *cond-mat/0203246*.
16. M. Zehetmayer, M. Eisterer, J. Jun, S. M. Kazakov, J. Karpinski, A. Wisniewski, and

- H. W. Weber, Phys. Rev. B **66**, 052505 (2002).
17. L. Lyard, P. Samuely, P. Szabo, C. Marcenat, T. Klein, K. H. P. Kim, C. U. Jung, H.-S. Lee, B. Kang, S. Choi, S.-I. Lee, L. Paulius, J. Marcus, S. Blanchard, A. G. M. Jansen, U. Welp, and W. K. Kwok, cond-mat/0206231.
 18. Y. Machida, S. Sasaki, H. Fujii, M. Furuyama, I. Kakeya, and K. Kadowaki, cond-mat/0207658.
 19. P. Miranović, K. Machida, and V. G. Kogan, cond-mat/0207146.
 20. This justifies our AGLT based analysis *a posteriori*. An only small deviation of the θ -dependence of H_{c2} from AGLT predictions (with a T dependent anisotropy) was also found in numerical calculations [25].
 21. P. A. Lee and S. R. Shenoy, Phys. Rev. Lett. **28**, 1025 (1972).
 22. U. Welp, S. Fleshler, W. K. Kwok, R. A. Klemm, V. M. Vinokur, J. Downey, B. Veal, and G. W. Crabtree, Phys. Rev. Lett. **67**, 3180 (1991).
 23. I. D. Lawrie, Phys. Rev. B **50**, 9456 (1994).
 24. D. R. Tilley, Proc. Phys. Soc. London **86**, 289 (1965), ; **86**, 678 (1965).
 25. P. Miranović *et al.*, unpublished.
 26. E. Helfand and N. R. Werthamer, Phys. Rev. **147**, 288 (1966).
 27. D. E. Farrell, C. M. Williams, S. A. Wolf, N. P. Bansal, and V. G. Kogan, Phys. Rev. Lett. **61**, 2805 (1988).
 28. D. Zech, C. Rossel, L. Lesne, H. Keller, S. L. Lee, and J. Karpinski, Phys. Rev. B **54**, 12535 (1996).
 29. V. G. Kogan, Phys. Rev. B **38**, 7049 (1988).
 30. V. G. Kogan, Phys. Rev. B **66**, 020509 (2002).
 31. A. A. Golubov, A. Brinkman, O. V. Dolgov, J. Kortus, and O. Jepsen, Phys. Rev. B **66**, 054524 (2002).
 32. F. Manzano and A. Carrington, Phys. Rev. Lett. **88**, 047002 (2002).
 33. In a very recent study, Kogan [V. G. Kogan, cond-mat/0207688] performed detailed calculations of the torque density from the free energy of the London model with different anisotropies γ_H and γ_λ . The obtained result is more complicated than the first approximation used in Ref. [34].
 34. J. Karpinski, M. Angst, J. Jun, S. M. Kazakov, R. Puzniak, A. Wisniewski, J. Roos, H. Keller, A. Perucchi, L. Degiorgi, M. Eskildsen, P. Bordet, L. Vinnikov, and A. Mironov, cond-mat/0207263.
 35. P. Szabó, P. Samuely, J. Kamarík, T. Klein, J. Marcus, D. Fruchart, S. Miraglia, C. Marcenat, and A. G. M. Jansen, Phys. Rev. Lett. **87**, 137005 (2001).
 36. F. Bouquet, Y. Wang, I. Sheikin, T. Plackowski, A. Junod, S. Lee, and S. Tajima, cond-mat/0207141.
 37. K. Takahashi, T. Atsumi, N. Yamamoto, M. Xu, H. Kitazawa, and T. Ishida, Phys. Rev. B **66**, 012501 (2002).
 38. M. Angst, R. Puzniak, A. Wisniewski, J. Roos, H. Keller, and J. Karpinski, cond-mat/0206407.
 39. X ray investigations of crystals B and C are in progress. Stacking faults have been observed in other samples of MgB₂, see, e.g., Y. Zhu, L. Wu, V. Volkov, Q. Li, G. Gu, A. R. Moodenbaugh, M. Malac, M. Suenaga, and J. Tranquada, Physica C **356**, 239 (2001).
 40. See, e.g., S. S. Banerjee, N. G. Patil, S. Ramakrishnan, A. K. Grover, S. Bhattacharya, P. K. Mishra, G. Ravikumar, T. V. C. Rao, V. C. Sahni, M. J. Higgins, C. V. Tomy, G. Balakrishnan, and D. M. Paul, Phys. Rev. B **59**, 6043 (1999).
 41. In the Bragg glass, the strong elastic forces disfavour non-collective pinning. Similar ideas were discussed in the context of cuprate superconductors with twin boundaries. See A. I. Larkin, M. C. Marchetti, and V. M. Vinokur, Phys. Rev. Lett. **75**, 2992 (1995).
 42. Similar observations were made on a YBa₂Cu₃O_{7- δ} crystal containing two twin boundaries. See W. K. Kwok, J. A. Fendrich, C. J. V. der Beek, and G. W. Crabtree, Phys. Rev. Lett. **73**, 2614 (1994).
 43. Ac susceptibility measurements were performed with a Quantum Design Physical Properties Measurement System with an excitation frequency of 10 kHz and amplitude $H_{ac} = 10$ Oe.
 44. R. Puzniak *et al.*, in preparation.

45. M. Pissas, S. Lee, A. Yamamoto, and S. Tajima, Phys. Rev. Lett. **89**, 097002 (2002).
46. G. P. Mikitik and E. H. Brandt, Phys. Rev. B **64**, 184514 (2001).
47. See, e.g., M. Angst, S. M. Kazakov, J. Karpinski, A. Wisniewski, R. Puzniak, and M. Baran, Phys. Rev. B **65**, 094518 (2002).